Optics Letters

# Cr:ZnS laser-pumped subharmonic GaAs optical parametric oscillator with the spectrum spanning 3.6–5.6 μm

V. O. Smolski,[1] S. Vasilyev,[2] P. G. Schunemann,[3] S. B. Mirov,[2,4] and K. L. Vodopyanov[1,*]

[1]CREOL, College of Optics and Photonics, University of Central Florida, Orlando, Florida 32816, USA
[2]IPG Photonics, Mid-IR Lasers, 1500 1st Ave N, Unit 39, Birmingham, Alabama 35203, USA
[3]BAE Systems, P.O. Box 868, MER15-1813, Nashua, New Hampshire 03061-0868, USA
[4]Department of Physics, University of Alabama Birmingham, CH 310, 1530 3rd Avenue South, Alabama 35294, USA
*Corresponding author: vodopyanov@creol.ucf.edu

Received 16 April 2015; revised 22 May 2015; accepted 28 May 2015; posted 29 May 2015 (Doc. ID 238245); published 15 June 2015

**Using a subharmonic optical parametric oscillator (OPO) based on orientation-patterned GaAs, we produced a broadband instantaneous output that spans 3.6–5.6 μm at 50-dB level (4.4–5.2 μm at 3 dB level), has 110 mW of average power, and is suitable for producing wideband-frequency combs in the mid-infrared. The OPO was synchronously pumped by a compact Kerr-lens mode-locked femtosecond Cr:ZnS oscillator with the central wavelength 2.38 μm and pulse repetition frequency 175 MHz.** 

***OCIS codes:*** (190.4975) Parametric processes; (190.4410) Nonlinear optics, parametric processes; (320.7110) Ultrafast nonlinear optics.

http://dx.doi.org/10.1364/OL.40.002906

Frequency combs in the region of fundamental vibrational resonances of molecules ($\lambda > 2.5$ μm) show great promise for high-resolution spectroscopy, trace molecular sensing, chemical standoff detection, hyperspectral imaging, and infrared nanospectroscopy [1–6]. Comb-based spectroscopy allows combining massive parallelism of data acquisition with high spectral resolution. Broad spectrum of the comb is critical for simultaneous detection of multiple molecular species. This effort extends the results of our earlier work on producing ultrabroadband mid-IR frequency combs via frequency-divide-by-two approach in a parametric nonlinear process.

The basic idea is to use a short (few-100-μm) second-order nonlinear crystal in a synchronously pumped optical parametric oscillator (OPO) operating at degeneracy. A variety of ultrafast lasers in combination with different $\chi^{(2)}$ nonlinear materials were used to attain this goal. For example, broadband (2.5–3.8 μm) instantaneous output was reported in a periodically poled lithium niobate (PPLN)-based OPO that was pumped by an Er-fiber laser [7], and 2.6–6.1-μm instantaneous span was achieved with an OPO based on orientation-patterned gallium arsenide (OP-GaAs) that was pumped by a Tm-fiber laser [8]. The key advantages of the degenerate OPO approach are low pump threshold due to double (signal and idler) resonance, potential for high (>60%) conversion efficiency due to nondissipative nature of parametric process [9], broadband OPO gain at degeneracy, and the fact that a doubly-resonant OPO inherits coherence properties of the pump laser [10,11].

Ultrafast $Cr^{2+}$:ZnS and $Cr^{2+}$:ZnSe lasers operating in the range of 2.3–2.5 μm are extremely well-suited for pumping GaAs-based subharmonic OPOs and potentially allow achieving > two octaves-wide frequency combs. The group velocity dispersion (GVD) for GaAs is small (~300 $fs^2/mm$) near OPO degeneracy (at 4.6–5 μm, twice the pump wavelength), and this results in a large parametric gain bandwidth that can be more than two octaves wide for a sufficiently thin (sub-mm) crystal. Additionally, small GVD is a prerequisite for the uniformity of mode spacing in the OPO resonator—a necessary condition for getting a broad frequency comb. On the other hand, vibronic $Cr^{2+}$:ZnS and $Cr^{2+}$:ZnSe lasers are considered to be mid-IR analogues of the Ti:sapphire laser—in terms of high emission cross-section, large gain bandwidth ($\Delta\lambda/\lambda > 35\%$, where $\Delta\lambda$ is the full width at half-maximum bandwidth), and capability of producing few-cycle pulses via ultrafast saturable absorbers and/or Kerr-lens mode locking. The most recent results include a Kerr-lens mode-locked polycrystalline $Cr^{2+}$:ZnS laser ($\lambda = 2.3$–$2.4$ μm) with the average power up to 2 W and pulse duration down to 29 fs (although not simultaneously) [12,13]. Using graphene-saturable absorber, pulses with 41-fs duration were produced in $Cr^{2+}$:ZnS at 2.4 μm [14]. Yet one more important advantage of Cr-doped ZnS/ZnSe lasers is that they allow, by analogy with Ti:sapphire lasers, producing frequency combs with large mode spacing, potentially 1–10 GHz—thanks to their compactness.

In the pioneering work on using vibronic $Cr^{2+}$ lasers for pumping GaAs OPOs, a mid-IR output centered at 4.9 μm was achieved with a 2.45-μm mode-locked Cr:ZnSe laser as a pump. With the utilizable pump power of 100 mW, the instantaneous spectral bandwidth of 1000 nm (30-dB level) and 500 nm (3-dB level), and the output power of 10 mW were

demonstrated [15]. Here we present our results on a Cr:ZnS-pumped broadband mid-IR OPO with almost 2-fold expansion of the spectral band and more than 10-fold increase in the average power, as compared to [15].

A Kerr-lens mode-locked Cr:ZnS laser with the central wavelength 2.38 μm, full width at half maximum (FWHM) bandwidth 60 nm, repetition rate 175 MHz, pulse duration 130 fs, and maximum average power 530 mW was used to synchronously pump the OPO. The ring-type OPO cavity (Fig. 1) was composed of a dielectric in-coupling mirror M1 ($CaF_2$ substrate) with high transmission (>95%) for the pump and high reflection for the OPO wavelengths (reflectivity >90% at 4.1–5.4 μm) and three gold-coated mirrors. Two of those mirrors (M2–M3) were parabolic with an off-axis angle 30° and radius of curvature in the apex R = 30 mm, and the third one, M4, was flat.

The OPO $\chi^{(2)}$ nonlinear gain medium was an orientation-patterned GaAs crystal grown at BAE Systems by a combination of molecular-beam and hydride vapor phase epitaxy. The crystal had a quasi-phase-matched (QPM) period of 92 μm, was 0.5 mm long, and kept at room temperature. The OP-GaAs was used at Brewster angle, and both the pump and the OPO signal/idler polarization directions were along ⟨111⟩ direction of GaAs. A wedged (0.5-deg) polished ~0.3 mm-thick $CaF_2$ plate was inserted into the cavity for (i) group velocity dispersion (GVD) compensation and (ii) the OPO beam outcoupling via Fresnel reflection. The OPO cavity was purged by dry nitrogen.

Parabolic mirrors were essential to minimize astigmatism in the OPO cavity. Typically, the astigmatic distortion introduced by a Brewster plate (GaAs in our case) is compensated by tilting spherical mirrors away from the normal [16]. Since the thickness of our GaAs is small, the compensating folding angle for spherical mirrors would be also small and that would cause clipping of the OPO beam, given the fact that the distance between the curved mirrors is small, ~30 mm. By choosing off-axis parabolas with the nominal folding angle of 30°, we were able to compensate GaAs astigmatism by a slight increase of the folding angle with respect to the nominal.

The OPO oscillates only when the doubly-resonant condition is met, which corresponds to discrete values of the cavity length separated (in terms of roundtrip) by approximately 2.4 μm (the pump wavelength) [7,8]. This condition was achieved by fine-tuning the cavity length with a piezo-actuator attached to the mirror M4. Generally, active locking (feedback to PZT) is needed to keep the OPO indefinitely in resonance.

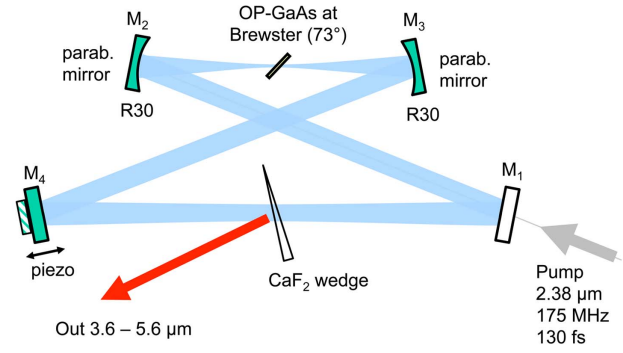


**Fig. 1.** Degenerate OP-GaAs optical parametric oscillator pumped by a $\lambda = 2.38$ μm ultrafast Cr:ZnS laser and formed by two flat and two off-axis parabolic mirrors. The OPO cavity was purged with dry nitrogen.

With no intentional outcoupling ($CaF_2$ plate at Brewster angle), the OPO threshold was measured to be 20 mW, and the average output power leaking from the mirror M1 (Fig. 1) was 26 mW at maximum pump. The measured pump depletion was as high as 92%, and the circulating OPO power (centered at ~4.8 μm) inside the cavity was estimated to be ~2 W. With the Fresnel outcoupling of 5% (counted as a sum of reflections from both $CaF_2$ surfaces) achieved by rotating the $CaF_2$ wedge toward normal incidence, we measured 110 mW of average power from the OPO (in two beams). The pump depletion in this case was 78% and the OPO threshold 144 mW.

The OPO power spectrum was measured using a grating monochromator and a cooled (77 K) MCT detector (Fig. 2). The spectrum is 2000 nm wide (3.6–5.6 μm) at 50-dB level and 800 nm wide (4.4–5.2 μm) at 3 dB. We believe that the spectral span was mostly limited by the reflectivity range of the in-coupling mirror (shown in Fig. 2). Moreover, because of imperfect purging, there might be a strong contribution from the atmospheric water absorption at $\lambda > 5$ μm (see top panel in Fig. 2).

An additional constraint on the frequency comb spectral width is imposed by intracavity group delay dispersion (GDD) which affects the uniformity of mode spacing of the OPO. Figure 3 depicts the computed GDD for 0.5-mm GaAs, for 0.3-mm $CaF_2$, and for the dielectric incoupling mirror (metallic mirrors produce negligible dispersion). One can see that GDD due to GaAs plus compensating $CaF_2$ plate is very low, and most of GDD comes from the dielectric mirror, again restricting the spectral span.

Thus we believe that all three factors: mirror reflectivity, mirror GDD, and atmospheric absorption—limit the instantaneous spectrum. In theory, the spectrum can be made much wider taking into account considerably broader GaAs

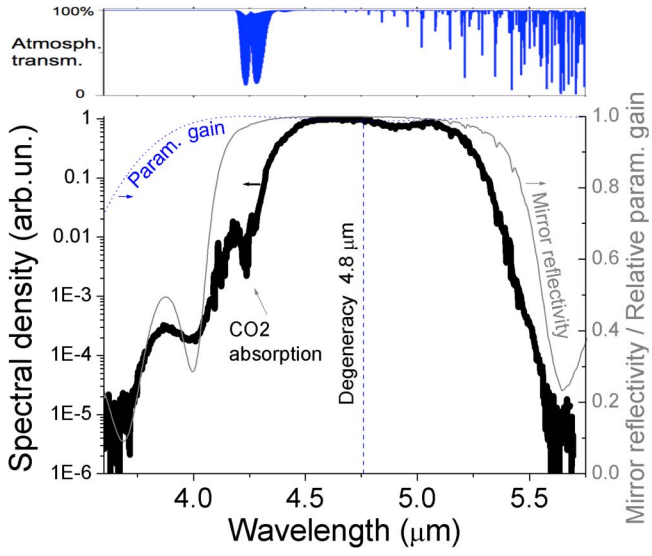


**Fig. 2.** OPO output spectrum. Also shown are reflectivity of the dielectric mirror M1 and normalized parametric gain of the OP-GaAs. Vertical dotted line is the OPO degeneracy (4.8 μm). The top panel shows transmission through 1.71 m (cavity roundtrip length) of the purged (~5% humidity) atmosphere, based on the HITRAN data.

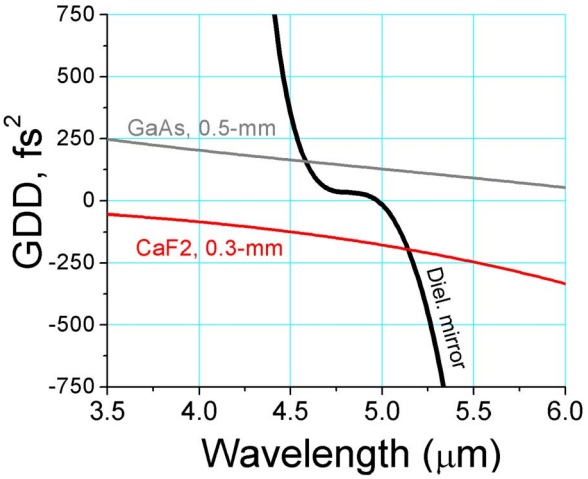


**Fig. 3.** Computed group delay dispersion (GDD) of different elements in the OPO cavity. Most of the GDD comes from the dielectric mirror.

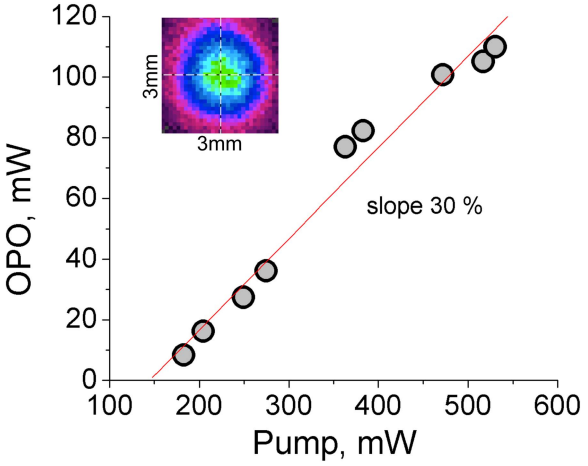


**Fig. 4.** Output–input characteristic of the OPO. The inset shows the OPO beam profile taken at 1-meter distance with a Spiricon Pyrocam III.

parametric gain bandwidth when pumped by a Cr:ZnS laser, as seen from Fig. 2.

Finally, Fig. 4 plots the output versus input power characteristic of the OPO. The slope efficiency is 30%, and there are no signs of roll-off, indicating that the three-photon absorption of the 2.38-μm pump in GaAs and other unwanted high-order effects play a minor role. The inset in Fig. 4 shows the OPO beam profile taken at 1-meter distance from the OPO outcoupler with a Spiricon pyroelectric camera. The beam size (~2 mm FWHM) is within ±5% of the diffraction limit.

In conclusion, without optimization of the outcoupling, we achieved 110 mW of average power from a subharmonic OP-GaAs OPO pumped by an ultrafast Cr:ZnS laser. The instantaneous spectral span of 3.6–5.6 μm was limited by the dielectric in-coupling mirror. The observed 78%–92% pump depletion indicates that at least 50% of the pump can be converted into the broadband OPO subharmonic, provided that an appropriate beam outcoupling is used. We should note here that the Cr:ZnS pump laser was operating far from the optimal regime. The laser was forced, with the use of an intracavity prism, to operate at 2.38 μm (dictated by the QPM period of the available OP-GaAs crystal), while much shorter (factor of 2) pulses and much higher (factor of 3) average power were available at 2.31 μm. With an appropriate QPM period of the OP-GaAs crystal, we expect to achieve the OPO output at a 0.5-W level. The next steps will include (i) using broadband dispersion-compensating dielectric mirrors and (ii) stabilizing carrier-envelope phase of the pump laser that will automatically result in the phase-stabilized subharmonic OPO comb.

Army Research Office (ARO) (A14A-006-0054); National Aeronautics and Space Administration (NASA) (NNX09AW13G); Office of Naval Research (ONR) (N00014-10-1-0281).

## REFERENCES

1. A. Schliesser, N. Picqué, and T. W. Hänsch, Nat. Photonics **6**, 440 (2012).
2. D. Mazzotti, P. Cancio, G. Giusfredi, P. De Natale, and M. Prevedelli, Opt. Lett. **30**, 997 (2005).
3. F. Adler, P. Maslowski, A. Foltynowicz, K. C. Cossel, T. C. Briles, I. Hartl, and J. Ye, Opt. Express **18**, 21861 (2010).
4. B. Bernhardt, E. Sorokin, P. Jacquet, R. Thon, T. Becker, I. T. Sorokina, N. Picque, and T. W. Hänsch, Appl. Phys. B **100**, 3 (2010).
5. Z. W. Zhang, T. Gardiner, and D. T. Reid, Opt. Lett. **38**, 3148 (2013).
6. M. Brehm, A. Schliesser, and F. Keilmann, Opt. Express **14**, 11222 (2006).
7. N. Leindecker, A. Marandi, R. L. Byer, and K. Vodopyanov, Opt. Express **19**, 6296 (2011).
8. N. Leindecker, A. Marandi, R. L. Byer, K. L. Vodopyanov, J. Jiang, I. Hartl, M. Fermann, and P. G. Schunemann, Opt. Express **20**, 7046 (2012).
9. K. A. Ingold, A. Marandi, C. Rudy, and R. L. Byer, "2.09-μm degenerate femtosecond OPO with over 60% conversion efficiency and 0.6-W output," in *CLEO Science and Innovations 2014*, Technical Digest (online) (Optical Society of America, 2014), paper SM2I.4.
10. A. Marandi, N. Leindecker, V. Pervak, R. L. Byer, and K. L. Vodopyanov, Opt. Express **20**, 7255 (2012).
11. K. F. Lee, J. Jiang, C. Mohr, J. Bethge, M. E. Fermann, N. Leindecker, K. L. Vodopyanov, P. G. Schunemann, and I. Hartl, Opt. Lett. **38**, 1191 (2013).
12. S. Mirov, V. Fedorov, D. Martyshkin, I. Moskalev, M. Mirov, and S. Vasilyev, IEEE J. Sel. Top. Quantum Electron. **21**, 292 (2015).
13. S. Vasilyev, M. Mirov, and V. Gapontsev, "Mid-IR Kerr-lens mode-locked polycrystalline $Cr^{2+}$:ZnS laser with 29 fs pulse duration," in *CLEO: 2015* (Optical Society of America, 2015), postdeadline paper JTh5C.3.
14. N. Tolstik, E. Sorokin, and I. T. Sorokina, Opt. Express **22**, 5564 (2014).
15. K. L. Vodopyanov, E. Sorokin, I. T. Sorokina, and P. G. Schunemann, Opt. Lett. **36**, 2275 (2011).
16. H. W. Kogelnik, E. P. Ippen, A. Dienes, and C. V. Shank, IEEE J. Quantum. Electron. **8**, 373 (1972).